

DEEP LEARNING AND ELICITABILITY FOR MCKEAN-VLASOV FBSDES WITH COMMON NOISE

FELIPE J. P. ANTUNES

School of Applied Mathematics, Getulio Vargas Foundation, Brazil

YURI F. SAPORITO

School of Applied Mathematics, Getulio Vargas Foundation, Brazil

SEBASTIAN JAIMUNGAL

*Department of Statistical Sciences, University of Toronto, Canada and
Oxford-Man Institute for Quantitative Finance, University of Oxford*

ABSTRACT. We present a novel numerical method for solving McKean-Vlasov forward-backward stochastic differential equations (MV-FBSDEs) with common noise, combining Picard iterations, elicibility and deep learning. The key innovation involves elicibility to derive a path-wise loss function, enabling efficient training of neural networks to approximate both the backward process and the conditional expectations arising from common noise — without requiring computationally expensive nested Monte Carlo simulations. The mean-field interaction term is parameterized via a recurrent neural network trained to minimize an elicitable score, while the backward process is approximated through a feedforward network representing the decoupling field. We validate the algorithm on a systemic risk interbank borrowing and lending model, where analytical solutions exist, demonstrating accurate recovery of the true solution. We further extend the model to quantile-mediated interactions, showcasing the flexibility of the elicibility framework beyond conditional means or moments. Finally, we apply the method to a non-stationary Aiyagari–Bewley–Huggett economic growth model with endogenous interest rates, illustrating its applicability to complex mean-field games without closed-form solutions.

1. INTRODUCTION

McKean-Vlasov Forward-Backward Stochastic Differential Equations (MV-FBSDEs) arise naturally in the study of stochastic control problems where the dynamics or cost functions depend on the law of the solution process. These equations combine the forward-backward structure characteristic of stochastic maximum principles with mean-field interactions through the law of the process. Formally, a MV-FBSDE system consists of a forward diffusion process

E-mail addresses: `felipe.antunes@fgv.br`, `yuri.saporito@fgv.br`, `sebastian.jaimungal@utoronto.ca`.

$(X_t)_{t \in [0, T]}$ coupled with backward processes $(Y_t, Z_t)_{t \in [0, T]}$, where the coefficients of the differential equations depend on both the current state and the law of X_t , typically, though not always, through its conditional moments. The coupling between the forward and backward components, together with the dependence on the law of the solution, make these equations particularly challenging from both theoretical and numerical perspectives. Of special interest is the case which the system is subject to common noise, introducing additional structure in the mean-field interaction through conditioning on a common source of randomness. Such systems play a fundamental role in the probabilistic analysis of mean-field games and mean-field type control problems, where they characterize Nash equilibria and optimal controls, respectively [CD+18].

The method we propose addresses two significant challenges in solving MV-FBSDEs with common noise: the forward-backward coupling and the dependence on the stochastic measure flow. We parameterize the mean-field term as a function of the common noise through an auxiliary recurrent neural network (to allow non-Markovian encoding), trained to minimize a score that elicits the required dependence on the measure flow. This approach eliminates the need for nested Monte Carlo simulation while maintaining adaptedness of the solution to the filtration generated by the common noise [CJC23].

We demonstrate the effectiveness of our method through numerical experiments on benchmark problems, showing particular advantages in the common noise case where traditional approaches struggle with computational efficiency. We also apply our proposed method to a more challenging MV-FBSDE arising from the economic growth model presented in [Ach+22].

A survey of numerical methods for BSDEs can be found in [Che+23], including methods using deep learning. A numerical method for MV-FBSDEs using recursive Picard iterations for small time intervals can be found in [CCD19]. Their method is based in splitting the time interval of the system into small time intervals, and calculating recursively empirical conditional expectations for Y at each time interval, whereas our method differs by performing a single Picard iteration for the whole time interval, using elicitability to calculate the conditional expectation for Y .

The works of [GMW22; ZOL24; HHL24] present various numerical methods for MV-FBSDEs using neural networks. [GMW22] uses deep learning to approximate Y , with the loss calculated over the terminal value Y_T . The mean field interaction is calculated empirically over sample paths. [ZOL24] proposes a method based on solving a characteristic system of ODEs. The method uses score functions and density estimation to avoid sampling from Brownian motions. [HHL24] uses deep learning to estimate the dependence on the law of the processes, then uses Deep BSDE to solve the backwards component. In comparison, our method uses elicitability to estimate the dependence on the law. This allows us to consider the case with common noise without costly sampling. Moreover, we use elicitability to solve for Y_t , creating a loss function defined over the whole time interval and allows us to easily incorporate mean-field interaction that go beyond moments, e.g., those that depend on quantiles or tail risk.

2. PROBLEM FORMULATION

We work on a complete probability space $(\Omega, \mathfrak{F}, \mathbb{P})$ on which we have two independent, d -dimensional Brownian motions $(W_t)_{t \in [0, T]}$ and $(W_t^0)_{t \in [0, T]}$ over a time horizon $T > 0$, where W^0 and W represent common and idiosyncratic noise, respectively. We denote the space of square-integrable \mathcal{A} -measurable random variables by $\mathbb{L}^2[\mathcal{A}]$ and adopt the following notation:

- ▷ $\mathcal{F}^0 = (\mathcal{F}_t^0)_{t \in \mathcal{T}}$, $\mathcal{F}_t^0 = \sigma(W_s^0, s \leq t)$, for the filtration generated by the common noise;
- ▷ $\mathcal{F} = (\mathcal{F}_t)_{t \in \mathcal{T}}$, $\mathcal{F}_t = \sigma(W_s, s \leq t)$, for the filtration generated by the idiosyncratic noise.

Our goal is to approximate the solution to the fully-coupled multidimensional MV-FBSDE describing the dynamics of $(X, Y) \in \mathbb{R}^\ell \times \mathbb{R}^m$:

$$dX_t = \mu(t, X_t, Y_t, Z_t, Z_t^0, S_t) dt + \sigma(t, X_t) dW_t + \sigma_0(t, X_t) dW_t^0, \quad X_0 = \xi, \quad (1)$$

$$dY_t = -f(t, X_t, Y_t, Z_t, Z_t^0, S_t) dt + Z_t^\top dW_t + Z_t^{0\top} dW_t^0, \quad Y_T = G(X_T, S_T), \quad (2)$$

where $\mu : [0, T] \times \mathbb{R}^\ell \times \mathbb{R}^m \times \mathbb{R}^{d \times m} \times \mathbb{R}^{d \times m} \times \mathbb{R}^p \rightarrow \mathbb{R}^\ell$, $\sigma : [0, T] \times \mathbb{R}^\ell \rightarrow \mathbb{R}^{\ell \times d}$, $\sigma_0 : [0, T] \times \mathbb{R}^\ell \rightarrow \mathbb{R}^{\ell \times d}$, $f : [0, T] \times \mathbb{R}^\ell \times \mathbb{R}^m \times \mathbb{R}^{d \times m} \times \mathbb{R}^{d \times m} \times \mathbb{R}^p \rightarrow \mathbb{R}^m$ and $G : \mathbb{R}^\ell \times \mathbb{R}^p \rightarrow \mathbb{R}^m$.

The quantity S_t is any elicitable, p -dimensional statistic (see [FZ16]) of the state X_t , conditioned on the path of the common noise up to time t , i.e. we assume there exists a *score function* \mathfrak{S} such that

$$S_t = \underset{\mathfrak{s} \in \mathbb{L}^2[\mathcal{F}_t^0]}{\operatorname{argmin}} \mathbb{E}[\mathfrak{S}(\mathfrak{s}, X_t)]. \quad (3)$$

Equivalently, S_t is an elicitable statistic of the conditional measure $\mu_t = \mathcal{L}(X_t | \mathcal{F}_t^0)$. For example, we may elicit conditional moments of X_t by choosing $\mathfrak{S}(\mathfrak{s}, x) = (\phi(x) - \mathfrak{s})^2$ and conditional α -quantiles of X_t by choosing $\mathfrak{S}(\mathfrak{s}, x) = (1_{\{\mathfrak{s} \geq x\}} - \alpha)(\mathfrak{s} - x)$. We provide further details on elicability in Section 2.2.2 below. This model falls into the setting of FBSDEs in a random environment, [CD+18, Chapter 1, Vol. II], in which such environment is given by the elicitable statistic $(S_t)_{t \in [0, T]}$.

We assume the initial condition ξ is in $\mathbb{L}^2[\mathcal{G}_0]$ and takes values in \mathbb{R}^ℓ , for a given initial information \mathcal{G}_0 . Furthermore, the full information, i.e. the filtration generated by both Brownian motions and the initial condition, is denoted by $\mathcal{G} = (\mathcal{G}_t)_{t \in \mathcal{T}}$, $\mathcal{G}_t = \mathcal{F}_t \vee \mathcal{F}_t^0 \vee \sigma(\xi)$. Below, we use $\|\cdot\|$ to denote the appropriate Euclidean norm.

Assumption 1 (Lipschitz Continuity). *To guarantee existence and uniqueness of solution for (1)–(2), we assume there exist $L, C, L_0 > 0$ such that the following properties hold:*

(i) *Linear growth:*

$$\|\mu(t, 0, 0, 0, 0, \mathfrak{s})\| + \|f(t, 0, 0, 0, 0, \mathfrak{s})\| + \|\sigma(t, 0)\| + \|\sigma_0(t, 0)\| \leq C(1 + \|\mathfrak{s}\|),$$

for all $t \in [0, T]$ and $\mathfrak{s} \in \mathbb{R}^p$;

(ii) *Lipschitz continuous coefficients:*

$$\begin{aligned} & \|\mu(t, x, y, z, z^0, \mathfrak{s}) - \mu(t, x', y', z', z'^0, \mathfrak{s})\| + \|f(t, x, y, z, z^0, \mathfrak{s}) - f(t, x', y', z', z'^0, \mathfrak{s})\| \\ & + \|\sigma(t, x) - \sigma(t, x')\| + \|\sigma_0(t, x) - \sigma_0(t, x')\| + \|G(x, \mathfrak{s}) - G(x', \mathfrak{s})\| \\ & \leq L(\|x - x'\| + \|y - y'\| + \|z - z'\| + \|z^0 - z'^0\|), \end{aligned}$$

for all $t \in [0, T]$ and $\mathfrak{s} \in \mathbb{R}^p$;

(iii) *Lipschitz continuous Y :*

$\|Y_t^{t,x} - Y_t^{t,x'}\| \leq L_0 \|x - x'\|$, for any $t \in [0, T]$ and $x, x' \in \mathbb{R}^\ell$, where $(X_s^{t,x}, Y_s^{t,x}, Z_s^{t,x}, Z_s^{0,t,x})_{s \in [t, T]}$ is a solution for (1)–(2) for deterministic initial condition x at time t .

Under Assumption 1, by [CD+18, Theorem 1.45, Proposition 1.52], there exists a unique solution $(X, Y, Z, Z^0)_{t \in [0, T]}$ for (1)–(2) such that

$$\mathbb{E} \left[\sup_{t \in [0, T]} \left\{ \|X_t\|^2 + \|Y_t\|^2 \right\} + \int_0^T \left(\|Z_t\|^2 + \|Z_t^0\|^2 \right) dt \right] < \infty. \quad (4)$$

Moreover, under Assumption 1, which will be a standing assumption henceforth, the backward process Y admits a representation of the form

$$Y_t = U(t, X_t, S_t), \quad (5)$$

for some function $U : [0, T] \times \mathbb{R}^\ell \times \mathbb{R}^p \rightarrow \mathbb{R}^m$ known as the *decoupling field* [CD+18, Proposition 1.46, Remark 1.49].

Integrating (2), we see that Y admits the following fixed-point representation

$$Y_t = \mathbb{E} \left[G(X_T, S_T) + \int_t^T f(u, X_u, Y_u, Z_u, Z_u^0, S_u) du \mid \mathcal{G}_t \right]. \quad (6)$$

We can rewrite this fixed-point representation using the elicitability of the mean (or equivalently the L^2 -projection representation for conditional expectations) via a quadratic score function:

$$Y_t = \operatorname{argmin}_{\mathfrak{Y} \in \mathbb{L}^2[\mathcal{G}_t]} \mathbb{E} \left[\left(\mathfrak{Y} - G(X_T, S_T) - \int_t^T f(u, X_u, Y_u, Z_u, Z_u^0, S_u) du \right)^2 \right]. \quad (7)$$

Moreover, by the decoupling field representation, we know that the minimizer in (7) must have the form $\mathfrak{Y}^* = U(t, X_t, S_t)$, and applying Itô's lemma and matching terms, we find

$$Z_t = \sigma(t, X_t)^\top \partial_x U(t, X_t, S_t), \quad (8)$$

The process Z^0 admits a similar representation using the Itô's formula along a flow of conditional measures [CD+18, Vol II, Theorem 4.17]. Using that representation for Z^0 , however, presents challenges for numerical implementation. Instead, in Section 2.2.4, we use another (approximate) representation that elicits it.

2.1. Proposed method. We next provide an overview of our methodology, and provide further details in Section 2.2. Our methodology proceeds iteratively. We fix a time discretization of $[0, T]$, denoted by $\mathcal{T} = \{t_0, \dots, t_N\}$, where $0 = t_0 < \dots < t_N = T$. Given samples of $(W_t, W_t^0)_{t \in \mathcal{T}}$ and initialization — which represents the initial guess for the solution to the MV-FBSDE system — $(X_t^0, Y_t^0, Z_t^0, Z_t^{0,0}, S_t^0)_{t \in \mathcal{T}}$, we update, at iteration $k \in \mathbb{N}$, each entry of $(X_t^k, Y_t^k, Z_t^k, Z_t^{0,k}, S_t^k)_{t \in \mathcal{T}}$ sequentially as follows:

- (i) First, we solve the forward SDE (1) for $(X_t^{k+1})_{t \in \mathcal{T}}$, through Picard iterations, with $(W_t, W_t^0)_{t \in \mathcal{T}}$ and $(Y_t^k, Z_t^k, Z_t^{0,k}, S_t^k)_{t \in \mathcal{T}}$ held fixed. We denote the n -th Picard iteration by $X_t^{k+1,n}$, set $X_t^{k+1,0} = X_t^k$, and repeat this inner Picard iteration until we achieve the desired convergence error in the L^2 -norm, say at iteration \mathfrak{n}_{k+1} . We then set $X^{k+1} = X^{k+1, \mathfrak{n}_{k+1}}$ resulting in the $(k+1)^{th}$ -outer Picard iteration of the process X .
- (ii) Next, using $(W_t, W_t^0)_{t \in \mathcal{T}}$ and $(X^{k+1})_{t \in \mathcal{T}}$, we compute S_t^{k+1} using elicitability, i.e. we solve the minimization problem (3) using X_t^{k+1} . We approximate $\mathfrak{s} \in \mathbb{L}^2[\mathcal{F}_t^0]$ as a recurrent neural network $\mathfrak{s}(t, (W_s^0)_{s \leq t})$, for $t \in \mathcal{T}$.
- (iii) Finally, with $(W_t, W_t^0)_{t \in \mathcal{T}}$, $(X_t^{k+1}, S_t^{k+1})_{t \in \mathcal{T}}$ and $(Y_t^k, Z_t^k, Z_t^{0,k})_{t \in \mathcal{T}}$ fixed, we solve for $(Y_t^{k+1}, Z_t^{k+1}, Z_t^{0,k+1})_{t \in \mathcal{T}}$ by calculating the conditional expectation for Y^{k+1} through elicitability using (7). We parameterize $Y_t^{k+1} \in \mathbb{L}^2[\mathcal{G}_t]$ as $U(t, X_t^{k+1}, S_t^{k+1})$ (the *decoupling field*) and approximate U as the output of a neural network. Finally, we obtain Z_t^{k+1} through automatic differentiation using the representation (8) and $Z_t^{0,k+1}$ using elicitability as described in Section 2.2.4.

Algorithm 1: Picard Iterations and Elicitability for MV-FBSDE

Input: Drift $\mu(u, x, y, z, z^0, s)$; diffusion coefficients $\sigma(u, x)$ and $\sigma_0(u, x)$; Initial condition X_0 ; Terminal condition $g(x, s)$; driver function $f(u, x, y, z, z^0, s)$; Time discretization \mathcal{T} ; Samples of $(W_t, W_t^0)_{t \in \mathcal{T}}$; Initial $(Y_t^0, Z_t^0, Z_t^{0,0}, S_t^0)_{t \in \mathcal{T}}$; Number of Picard iterations K .

Output: Samples of $(X_t^K, Y_t^K, Z_t^K, Z_t^{0,K}, S_t^K)_{t \in \mathcal{T}}$ providing an approximate solution to the system (1)-(2); Trained neural networks $S_\theta, U_\theta, v_\theta$.

```

1 for  $k = 1$  to  $K$  do
2   Given  $(X_t^k, Y_t^k, Z_t^k, Z_t^{0,k}, S_t^k)_{t \in \mathcal{T}}$ , use Algorithm 2 to sample  $(X_t^{k+1})_{t \in \mathcal{T}}$  ;
3   Given  $(X_t^{k+1})_{t \in \mathcal{T}}$ , use Algorithm 3 to sample  $(S_t^{(k+1)})_{t \in \mathcal{T}}$  ;
4   Given  $(X_t^{k+1}, Y_t^k, Z_t^k, Z_t^{0,k}, S_t^{k+1})_{t \in \mathcal{T}}$ , use Algorithm 4 to sample  $(Y_t^{k+1}, Z_t^{k+1})_{t \in \mathcal{T}}$  ;
5   Given  $(X_t^{k+1}, Y_t^{k+1}, Z_t^{k+1}, Z_t^{0,k}, S_t^{k+1})_{t \in \mathcal{T}}$ , use Algorithm 5 to sample  $(Z_t^{0,k+1})_{t \in \mathcal{T}}$ .
6 return Samples of  $(X_t^K, Y_t^K, Z_t^K, Z_t^{0,K}, S_t^K)_{t \in \mathcal{T}}$ 

```

These steps are summarized in Algorithm 1 and the code is available at https://github.com/fjpAntunes/mean-field-tools/tree/main/mean_field_tools/deep_bsde.

To improve convergence and stability of the algorithm, we dampen the full iteration by performing ‘soft-updates’ of the processes as follows

$$\Psi^{k+1} = \delta \Psi^k + (1 - \delta) \hat{\Psi}^{k+1}, \quad (9)$$

where Ψ is X, Y, Z and Z^0 and $0 < 1 - \delta \ll 1$ is a damping coefficient and hatted variables represent the updates computed from the steps above.

We continue the main outer iteration until a maximum number of iterations is reached, or the \mathbb{L}^2 -norm between samples of successive iterations of X, Y, Z and Z^0 fall below a specified tolerance.

2.2. Detailed description. We next provide a detailed description of our methodology. As outlined above, our method consists in iterating between fixing the backward SDE and solving the forward SDE by Picard iterations, and fixing the forward SDE and solving the BSDE by elicibility. Each step of this process consists in a Picard iteration for the whole MV-FBSDE system. The MV aspect requires estimating S_t , which is achieved by elicibility as well.

We remind the reader that the outer-Picard iteration of the backward SDE is indexed by k and, for each k , the inner-Picard iteration of the forward SDE is indexed by n .

2.2.1. Solving the forward SDE by Picard iterations. Suppose we are at the k^{th} outer iteration, i.e., $(X^k, Y^k, Z^k, Z^{0,k}, S^k)$ are fixed. We define $X^{k+1,n}$ to be the n^{th} -inner Picard update of the forward process. To this end, set $X^{k+1,0} = X^k$, and given $X^{k+1,n}$, we obtain $X^{k+1,n+1}$ through

$$\begin{aligned} X_t^{k+1,n+1} = & X_0 + \int_0^t \mu(u, X_u^{k+1,n}, Y_u^k, Z_u^k, Z_u^{0,k}, S_u^k) \, du \\ & + \int_0^t \sigma(u, X_u^{k+1,n}) \, dW_u + \int_0^t \sigma_0(u, X_u^{k+1,n}) \, dW_u^0, \end{aligned}$$

by numerically evaluating the right-hand side using Euler-Maruyama method with time discretization \mathcal{T} until $\|X^{k+1,n+1} - X^{k+1,n}\|_{\mathbb{L}^2(\Omega \times [0, T])}$ is below a specified tolerance; see Algorithm 2 for a pseudo-code, where we have suppressed the outer iteration counter, k , for simplicity.

Algorithm 2: Picard iteration of forward SDE with fixed (Y, Z, Z^0, m)

Input: Drift $\mu(u, x, y, z, z^0, s)$; diffusion coefficients $\sigma(u, x)$ and $\sigma_0(u, x)$; Initial condition X_0 ; Time discretization \mathcal{T} ; Tolerance parameter ε ; M samples of $(W_t, W_t^0)_{t \in \mathcal{T}}$; samples of $(Y_t, Z_t, Z_t^0, S_t)_{t \in \mathcal{T}}$.

Output: M samples of $(X_t)_{t \in \mathcal{T}}$ at the next Picard iteration.

```

1 Initialize  $X_t^0 \equiv X_0$ 
2  $n \leftarrow 0$ ;
3 while  $\epsilon \geq \varepsilon$  do
4   Using Euler-Maruyama in  $\mathcal{T}$ , approximate  $M$  samples of
      
$$X_t^{n+1} = X_0 + \int_0^t \mu(u, X_u^n, Y_u, Z_u, Z_u^0, S_u) \, du + \int_0^t \sigma(u, X_u^n) \, dW_u + \int_0^t \sigma_0(u, X_u^n) \, dW_u^0;$$

      Compute error
      
$$\epsilon = \frac{1}{MN} \sum_{j=1}^N \sum_{i=1}^M \|X_{t_j}^{n+1(i)} - X_{t_j}^{n(i)}\|^2;$$

       $n \leftarrow n + 1$ ;
5 return  $X^{n+1}$ 
```

2.2.2. Estimating S through elicitability. Elicitability provides a framework for computing statistics through minimization of scoring functions [FZ16]. For example, given a random variable X taking values in \mathbb{R} , and a σ -algebra \mathcal{G} , the conditional expectation $\mathbb{E}[X | \mathcal{G}]$ can be characterized as the minimizer of the L^2 loss:

$$\mathbb{E}[X | \mathcal{G}] = \operatorname{argmin}_{Y \in \mathbb{L}^2(\mathcal{G})} \mathbb{E}[(X - Y)^2]. \quad (10)$$

This characterization transforms the problem of computing conditional expectations into an minimization problem over \mathcal{G} -measurable random variables with second moment.

At the k^{th} outer iteration, we have samples from $(X^k, Y^k, Z^k, Z^{0,k}, S^k)_{t \in \mathcal{T}}$ and in the previous section, we have obtained samples from $(X^{k+1})_{t \in \mathcal{T}}$. We will next estimate S^{k+1} .

We begin by analyzing the cases where the dependency on S is through some conditional moment $S_t = \mathbb{E}[\phi(X_t) | \mathcal{F}_t^0]$. When there is no common noise, S_t^{k+1} can be estimated by calculating the empirical average over samples of $\phi(X_t^{k+1})$. In the case where there is common noise this would be numerically prohibited, as we need to condition on the state of common noise. Instead, we use elicitability and rewrite the conditional expectation as a minimization problem

$$S_t^{k+1} = \operatorname{argmin}_{s \in \mathbb{L}^2(\mathcal{F}_t^0)} \mathbb{E}[(\phi(X_t^{k+1}) - s)^2]. \quad (11)$$

More generally, if S_t is any elicitable statistic for a score function \mathfrak{S} over the conditional probability measure of X_t given \mathcal{F}_t^0 , we may write

$$S_t^{k+1} = \operatorname{argmin}_{s \in \mathbb{L}^2(\mathcal{F}_t^0)} \mathbb{E}[\mathfrak{S}(X_t^{k+1}, s)]. \quad (12)$$

For example, we may elicit the (conditional) α -quantile by using the score function

$$\mathfrak{S}(x, s) = (1_{\{x \geq s\}} - \alpha)(x - s). \quad (13)$$

On the other hand, α -expected shortfall is not elicitable on its own, but it is 2-elicitable, meaning α -quantile and α -expected shortfall are jointly elicitable. A brief exposition of elicitability can be found in [Pes+24].

In general, the solution of the optimization (12) may not be Markovian in W^0 . Therefore, we consider a *recurrent* neural network (RNN) to the parametrize the function S , and find an approximate solution for the minimization problem (11) through stochastic gradient descent. See Algorithm 3 for a pseudo-code, where we suppress the outer iteration counter, k , for simplicity.

Algorithm 3: Estimating S through elicitability for fixed (X, Y, Z, Z^0)

Input: Score function \mathfrak{S} to elicit S ; M samples of $(W_t, W_t^0)_{t \in \mathcal{T}}$; M samples of $(X_t)_{t \in \mathcal{T}}$; Batch size I ; number of iterations E .

Output: M samples of $(S_t)_{t \in \mathcal{T}}$ with respect to the input samples of $(X_t)_{t \in \mathcal{T}}$ and $(W_t^0)_{t \in \mathcal{T}}$; Trained recurrent neural network S_θ .

```

1 Initialize recurrent neural network  $S_\theta$  with random weights  $\theta$ ;
2 for  $iter = 1$  to  $E$  do
3   sample  $I$  indexes  $\{k_1, \dots, k_I\}$  from  $\{1, \dots, M\}$  with replacement.
4   Compute loss:
5   
$$L(\theta) = \frac{1}{IN} \sum_{t \in \mathcal{T}} \sum_{i=1}^I \mathfrak{S}(X_t^{(k_i)}, S_\theta(t, (W_s^{0(k_i)})_{u \leq t, u \in \mathcal{T}}));
6   Update  $\theta$  using Adam;
7 return Trained recurrent neural network  $S_\theta$$$

```

2.2.3. Solving the backward SDE through elicitability. Given $(X^k, Y^k, Z^k, Z^{0,k}, S^k)$, from the previous two steps have estimated X^{k+1} and S^{k+1} , we next update Y . Based on the representation (7), we consider the following minimization problem:

$$Y_t^{k+1} = \underset{\mathfrak{Y} \in \mathbb{L}^2[\mathcal{G}_t]}{\operatorname{argmin}} \mathbb{E} \left[\left(\mathfrak{Y} - \left(G(X_T^{k+1}, S_T^{k+1}) + \int_t^T f(u, X_u^{k+1}, Y_u^k, Z_u^k, Z_u^{0,k}, S_u^{k+1}) du \right) \right)^2 \right]. \quad (14)$$

The structure given by the decoupling field in Equation (5) implies that we may parameterize the backward process Y using a neural network that takes (t, X_t, S_t) as inputs.

Our numerical method consists in finding an approximate solution for the minimization problem (14). Denote the numerical solution of this minimization procedure by U_θ . Hence, we set $Y_t^{k+1} = U_\theta(t, X_t^{k+1}, S_t^{k+1})$. To improve convergence rates, we calculate the loss with time dependent weights p_t , using a higher weight to the terminal condition - typically, $p_T = \frac{N}{2}$ and $p_t = 1$ for $t < T$. We provide a summary of this part of the method in Algorithm 4, where we have suppressed the counter k for simplicity and we are using θ to represent the generic neural network parameters throughout the paper.

2.2.4. Approximating Z and Z_0 . We obtain Z_t^{k+1} through automatic differentiation using the representation given in (8):

$$Z_t^{k+1} = \sigma(t, X_t^{k+1})^\top \nabla_x U_\theta(t, X_t^{k+1}, S_t^{k+1}). \quad (15)$$

A similar representation for Z^0 would require computing the Lyons derivative of U , which is numerically prohibitive. Moreover, while Y , and hence Z , depend of the conditional law of X only through S , Z^0 may depend fully on μ . Hence, we consider the following discretization of the backward dynamics of Y (2) in the discretized times \mathcal{T} :

$$\Delta Y_j^{k+1} := Y_{t_{j+1}}^{k+1} - Y_{t_j}^{k+1} \approx -f_j^{k+1} (t_{j+1} - t_j) + Z_{t_j}^{k+1 \top} \Delta W_j + Z_{t_j}^{0,k \top} \Delta W_j^0, \quad (16)$$

Algorithm 4: Estimating Y through elicability with fixed (X, Z, Z^0, m)

Input: Terminal condition g ; driver function $f(u, x, y, z, z^0, s)$; Time discretization \mathcal{T} ; weights p_t and sum of weights $P = \sum_{t \in \mathcal{T}} p_t$; M samples of $(W_t, W_t^0)_{t \in \mathcal{T}}$; M samples of $(X_t, S_t)_{t \in \mathcal{T}}$ at the next Picard iteration; M samples $(Y_t, Z_t, Z_t^0)_{t \in \mathcal{T}}$ at the current Picard iteration; Batch size I ; number of iterations E .

Output: M samples of $(Y_t, Z_t)_{t \in \mathcal{T}}$ at the next Picard iteration; Trained neural network U_θ .

1 Initialize neural network U_θ with random weights θ ;

2 **for** $iter = 1$ to E **do**

3 sample I indexes $\{k_1, \dots, k_I\}$ from $\{1, \dots, M\}$ with replacement.

4 Set $f_u = f(u, X_u, Y_u, Z_u, Z_u^0, S_u)$, for $u \in \mathcal{T}$;

5 Compute the loss

$$\mathcal{L}(\theta) = \frac{1}{IP} \sum_{t \in \mathcal{T}} \sum_{i=1}^I p_t \left(U_\theta(t, X_t^{(k_i)}, S_t^{(k_i)}) - G(X_T^{(k_i)}, S_T^{(k_i)}) - \sum_{u \in \mathcal{T}, u \geq t} f_u^{(k_i)} \Delta t \right)^2;$$

6 Update θ using Adam;

6 **return** Trained neural network u_θ

where, for $j = 0, \dots, N - 1$, $f_j^{k+1} = f(t_j, X_{t_j}^{k+1}, Y_{t_j}^{k+1}, Z_{t_j}^{k+1}, Z_{t_j}^{0,k}, S_{t_j}^{k+1})$. We may then update $Z_{t_j}^0$ by computing

$$Z_{t_j}^{0,k+1} = \mathbb{E} \left[\left. \left(\frac{\Delta Y_j^{k+1}}{\Delta t} + f_j^{k+1} \right) \Delta W_j^0 \right| \mathcal{G}_{t_j} \right]. \quad (17)$$

Thus, as we have samples of $(Y_t^{k+1})_{t \in \mathcal{T}}$ and $(f_t^{k+1})_{t \in \mathcal{T}}$ from the previous steps, we may elicit $Z^{0,k+1}$ by

$$Z_{t_i}^{0,k+1} = \underset{\mathfrak{Z} \in \mathbb{L}^2[\mathcal{G}_{t_i}]}{\operatorname{argmin}} \mathbb{E} \left[\left. \left(\mathfrak{Z} - \left(\frac{\Delta Y_i^{k+1}}{\Delta t} + f_i^{k+1} \right) \Delta W_i^0 \right)^2 \right] . \quad (18)$$

We provide a summary of this part of the method in Algorithm 5. As we mentioned, in general, Z^0 might depend fully on μ . Hence, we parametrize Z^0 as a recurrent neural network that takes $(t, X_t, (W_s^0)_{s \leq t})$ as inputs, to encode this path-dependence.

Algorithm 5: Estimating Z^0 through elicability with fixed (X, Y, Z, m)

Input: Driver function $f(u, x, y, z, z^0, s)$; Time discretization \mathcal{T} ; M samples of $(W_t, W_t^0)_{t \in \mathcal{T}}$; M samples of $(X_t, S_t, Y_t, Z_t)_{t \in \mathcal{T}}$ at the next Picard iteration; M samples of $(Z_t^0)_{t \in \mathcal{T}}$ at the current Picard iteration; Batch size I ; number of iterations E .

Output: M samples of $(Z_t^0)_{t \in \mathcal{T}}$ at the next Picard iteration; Trained recurrent neural network v_θ .

1 Initialize recurrent neural network v_θ with random weights θ ;

2 **for** $iter = 1$ to E **do**

3 sample I indexes $\{k_1, \dots, k_I\}$ from $\{1, \dots, M\}$ with replacement.

4 Set $f_u = f(u, X_u, Y_u, Z_u, Z_u^0, S_u)$;

5 Calculate $\Delta Y_t^{(k_i)} := Y_{t+\Delta t}^{(k_i)} - Y_t^{(k_i)}$ Compute the loss

$$\mathcal{L}(\theta) = \frac{1}{IN} \sum_{t \in \mathcal{T} \setminus \{T\}} \sum_{i=1}^I \left(v_\theta(t, X_t^{(k_i)}, (W_s^{0(k_i)})_{s \leq t, s \in \mathcal{T}}) - \left(\frac{\Delta Y_t^{(k_i)}}{\Delta t} + f_t^{(k_i)} \right) \Delta W_t^{0(k_i)} \right)^2;$$

6 Update θ using Adam;

6 **return** Trained recurrent neural network v_θ

2.3. Sampling after training. After completing Algorithm 1 to the desired accuracy, we have approximate samples of the processes (X, Y, Z, Z^0, S) over the discretized times \mathcal{T} . Moreover, as a product of the algorithm, we also have neural networks to approximately sample Y, Z, Z^0 , given samples of (W, W^0) and X . Therefore, if one wishes to sample the full set of processes (X, Y, Z, Z^0, S) after training, it may be done by discretizing the forward dynamics (1), as described in Algorithm 6.

Algorithm 6: Approximate samples of MV-FBSDE after training

Input: Drift $\mu(u, x, y, z, z^0, s)$; diffusion coefficients $\sigma(u, x)$ and $\sigma_0(u, x)$; Initial condition X_0 ; Time discretization \mathcal{T} ; Samples of $(W_t, W_t^0)_{t \in \mathcal{T}}$.

Output: Approximate samples $(X_t, Y_t, Z_t, Z_t^0, S_t)_{t \in \mathcal{T}}$

- 1 Set $S_u^\theta = S_\theta(u, (W_s^0)_{s \leq u})$ and $z_\theta(u, x, s) = \sigma(u, x)^\top \nabla_x U_\theta(u, x, s)$;
- 2 Using Euler-Maruyama in \mathcal{T} , approximate M samples of

$$X_t = X_0 + \int_0^t \mu(u, X_u, U_\theta(u, X_u, S_u^\theta), z_\theta(u, X_u, S_u^\theta), v_\theta(u, X_u, (W_s^{0(i)})_{s \leq u}), S_u^\theta) \, du \\ + \int_0^t \sigma(u, X_u) \, dW_u + \int_0^t \sigma_0(u, X_u) \, dW_u^0;$$

- 3 **return** Samples of $(X_t, U_\theta(t, X_t, S_t^\theta), z_\theta(t, X_t, S_t^\theta), v_\theta(t, X_t, (W_s^{0(i)})_{s \leq t}), S_\theta(t, (W_s^0)_{s \leq t}))_{t \in \mathcal{T}}$

3. NUMERICAL EXPERIMENTS

In this section, we present numerical experiments to demonstrate the effectiveness of our methodology. The first experiment solves the systemic risk banking model introduced in [CFS15]. This model can be solved analytically, hence it is useful as a benchmark against our numerical methodology. Building on this foundation, our second experiment modifies the systemic risk model by replacing interaction through the *mean* of the agents for an interaction through a *quantile* of the population. Finally, our third experiment solves a non-stationary Aiyagari–Bewley–Huggett model of income and wealth distribution [Ach+22], where the mean field interaction is mediated through the interest rate and the agents are subjected to a common noise.

All experiments have the following neural network configuration:

- ▷ Y Neural net: 2 layers, 18 nodes per layer, Feed Forward.
- ▷ Z^0 neural net: a single GRU layer with a 2-dimensional hidden node, followed by a single Feed Forward layer for output.
- ▷ S neural net: a single GRU layer with a 2-dimensional hidden node, followed by a single Feed Forward layer for output.

These NNs are small compared with many choices one can make, however, for the numerical experiments we investigate below, they prove to be expressive enough to approximate the solutions well.

Each Picard iteration consists of $E = 1,000$ backpropagation iterations for the Y neural net, $E = 500$ iterations for the Z^0 neural net, $E = 1,000$ iterations for the S neural net, using batches of $I = 2,048$ paths. We use the Adam optimizer with learning rate 0.005 and a decay each 5 steps of 0.9997. Soft updates of neural networks in (9) are performed with $\delta = 0.5$, following the fictitious play methodology described in [Lau21]. Moreover, we discretize the time interval in $N = 101$ timesteps, sample $M = 10,000$ paths to train the neural networks, and we perform $K = 20$ (outer) Picard iterations. Each (outer) Picard iteration takes approximately 22 seconds to execute on a T4 machine in Google Colab.

3.1. Systemic risk banking model.

3.1.1. *Problem formulation.* As the model presented in [CFS15] is linear-quadratic, it admits an explicit solution and hence provides useful testing ground. In the model, each bank controls its rate of borrowing/lending to a central bank. The state X_t represents the log-monetary reserve of a representative bank, which reverts to the mean log-monetary reserve S_t . The Nash equilibrium is characterized by the solution to the MV-FBSDE system

$$\begin{cases} dX_t = [(a + q)(S_t - X_t) - Y_t] dt + \sigma dB_t, & X_0 = \xi, \\ dY_t = [(a + q)Y_t + (\epsilon - q^2)(S_t - X_t)] dt + Z_t dW_t + Z_t^0 dW_t^0, & Y_T = c(X_T - S_T), \end{cases} \quad (19)$$

where $B_t = \rho W_t^0 + \sqrt{1 - \rho^2} W_t$ and S is the conditional mean:

$$S_t = \mathbb{E}[X_t | \mathcal{F}_t^0]. \quad (20)$$

The analytic solution for Y_t is

$$Y_t = -\eta(t)(S_t - X_t), \quad (21)$$

where η is the solution to the Riccati ODE

$$\dot{\eta}(t) = 2(a + q)\eta(t) + \eta^2(t) - (\epsilon - q^2), \quad (22)$$

which is given by

$$\eta(t) = \frac{-(\epsilon - q^2) \left(e^{(\delta^+ - \delta^-)(T-t)} - 2 \right) - c \left(\delta^+ e^{(\delta^+ - \delta^-)(T-t)} - \delta^- \right)}{(\delta^- e^{(\delta^+ - \delta^-)(T-t)} - \delta^+) - c \left(e^{(\delta^+ - \delta^-)(T-t)} - 1 \right)}, \quad (23)$$

with

$$\delta^\pm = -(a + q) \pm \sqrt{(a + q)^2 + (\epsilon - q^2)}. \quad (24)$$

Hence, the dynamics for X_t may be written

$$dX_t = [(a + q + \eta(t))(S_t - X_t)] dt + \sigma dB_t, \quad X_0 = \xi. \quad (25)$$

Applying conditional expectations on the common noise on (25), we conclude that $S_t = \mathbb{E}[\xi] + \rho \sigma W_t^0$. Using the integrating factor $\Theta(t) = \int_0^t \theta(s) ds$, where $\theta(t) = a + q + \eta(t)$, the complete analytical solution for the MV-FBSDE is given by

$$\begin{cases} S_t = \mathbb{E}[\xi] + \rho \sigma W_t^0, \\ X_t = \xi e^{-\Theta(t)} + \int_0^t \theta(u) S_u e^{-(\Theta(t) - \Theta(u))} du + \sigma \int_0^t e^{-(\Theta(t) - \Theta(u))} dB_u, \\ Y_t = -\eta(t)(S_t - X_t), \\ Z_t = \sigma \eta(t), \\ Z_t^0 = 0. \end{cases} \quad (26)$$

3.1.2. *Numerical simulation and parameters.* For numerical experiments, we choose parameters values that appear in [CFS15]: $a = q = c = \sigma = 1$, $\epsilon = 10$, and $\rho = 0.3$. The initial condition ξ is sampled from the normal distribution with mean 0 and variance 4.

Figure 1 shows a comparison between approximated and analytical solutions for two realizations, while, in Figure 2, we show a sample path as the outer Picard iterations evolve.

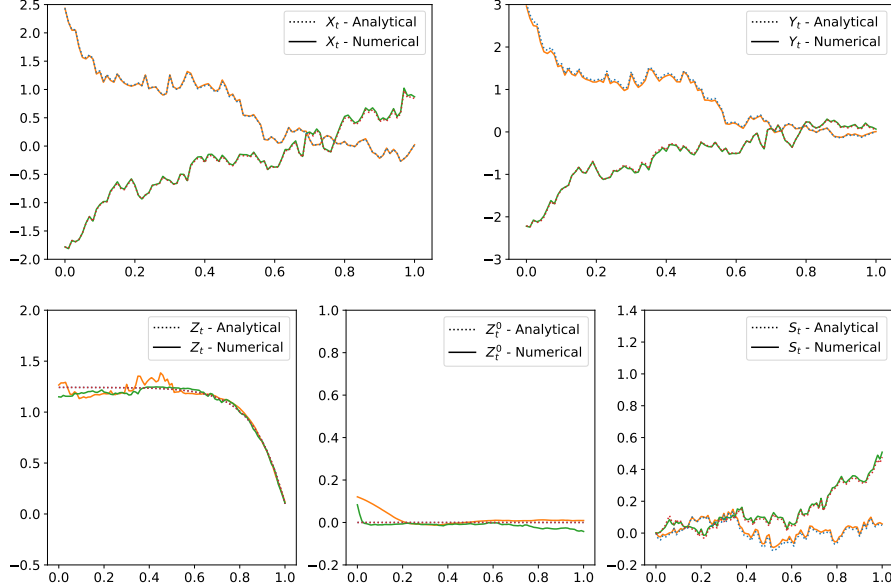


FIGURE 1. Comparison between analytic solution and approximated solution on two sample paths for the systemic risk with common noise experiment. Solid lines are the numerical solutions, and dotted lines represent the analytical solution. Each color pair (orange and blue, green and red) represents a particular path of each variable of the system.

3.2. Interaction through quantile. To test our algorithm in more challenging example, we apply the algorithm to a modified version of system (19) where the interaction term S_t is the α -quantile, with $\alpha = 60\%$, see Equation (13). We use the same values for all other parameters.

Figure 3 shows two sample paths of the variables at Nash equilibrium, along with the elicited quantile $\alpha = 60\%$. The sample paths are subjected to the same Brownian motions W_t and W_t^0 as in Figure 1. We can observe an upwards shift in the measure flow, when compared with the case where the interaction is through the mean. Intuitively, when every agent strives to be better than average, the population as a whole drifts upwards.

3.3. Economic growth model.

3.3.1. Problem formulation. Our next example examines the limit of a stochastic economy with N agents who make consumption-savings decisions over a finite time horizon, such as those described in [Ach+22], when N goes to infinity. Each agent starts with random initial capital k^i and chooses their consumption rate to maximize a given utility. The capital dynamics depend on consumption, depreciation, and an endogenous interest rate determined by aggregate capital in the economy. This creates strategic interaction through the interest rate — each individual agent's optimal consumption depends on the aggregate capital level, while the aggregate capital

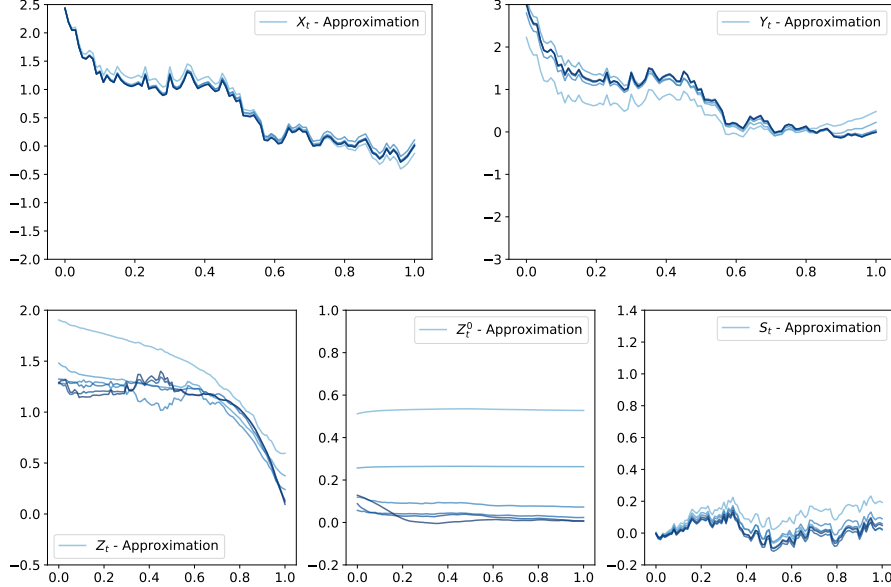


FIGURE 2. The same sample path at iterations 1,2,4,8,16 and 32. As iteration increases, the color becomes darker.

evolves based on all agents' consumption choices. We then consider the mean field limit with a continuum of agents distributed according to a probability measure flow. The Nash equilibrium is then characterized by an MV-FBSDE system. The model demonstrates how individual optimization and aggregate dynamics couple through the interest rate mechanism.

Consider an idealized economy where the i th agent capital dynamics, denoted K_t^i , is governed by two factors in addition to their consumption c^i : a fixed depreciation rate δ and an endogenous interest rate r_t . Moreover, it is subjected to an idiosyncratic noise W^i and a common noise W^0 that affects all agents. The dynamics is described by the SDE:

$$dK_t^i = ((r_t - \delta) K_t^i - c_t^i) dt + \sigma(\rho dW_t^0 + \sqrt{1 - \rho^2} dW_t^i), \quad K_0^i = k^i. \quad (27)$$

We further assume that the economy's aggregate production P_t is given by a function F of the aggregate capital of the economy \bar{K}_t , that is,

$$P_t = F(\bar{K}_t), \quad \text{where } \bar{K}_t = \frac{1}{N} \sum_{i=1}^N K_t^i. \quad (28)$$

In economic equilibrium, the interest rate r_t is given by the marginal effect of capital $\partial_K P$ in the aggregate production, which itself is a function of the aggregate capital in the economy \bar{K}_t . This is the source of the mean field interactions in this model.

The agents' consumption preferences are governed by the utility function $u(\cdot)$, and their preference for capital at the end of the time horizon are governed by a terminal utility $\psi(K_T^i)$.

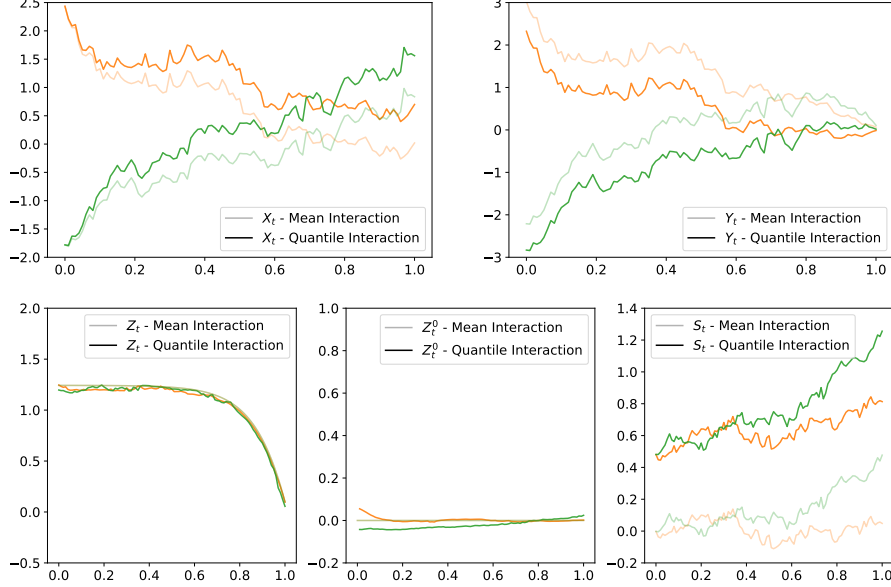


FIGURE 3. Modified systemic risk model where interaction is mediated through the 60% quantile. Respective paths (subjected to the same Brownian motion) of the original, mean interaction systemic risk model are shown in lighter shades. Note that the X_t variable is greater in the quantile interaction model.

Therefore, agents choose their consumption $c : [0, T] \times \Omega \rightarrow C$, with $C \subset \mathbb{R}$, to maximize the following functional:

$$J^i(k^i, c^i) = \mathbb{E} \left[\int_0^T u(c_t^i) dt + \psi(K_T^i) \right], \quad (29)$$

where k^i is the initial capital and K_T^i is their capital at time T when following the control process c^i , and assumed to be sufficiently regular so the functional above is well defined. In all, the optimization problem faced by agent i is

$$\begin{cases} \max_{c^i \geq 0} \mathbb{E} \left[\int_0^T u(c_s^i) ds + \psi(K_T^i) \right], \\ \text{subject to} \\ dK_t^i = [(\partial_K F(\bar{K}_t) - \delta) K_t^i - c_t^i] dt + \sigma(\rho dW_t^0 + \sqrt{1 - \rho^2} dW_t^i), \quad K_0^i = k^i. \end{cases} \quad (30)$$

We next choose logarithmic utility $u(c) = \log(c)$, and then we assume the consumption takes values in the positive reals $C = \mathbb{R}_+$. Moreover, we consider quadratic terminal cost $\psi(K) = -\frac{1}{2}K^2$, and quadratic aggregation function $F(K) = \frac{C}{2}K^2$. With these choices, the optimal consumption is given by $c_t^* = 1/Y_t$. In the mean-field limit, we denote the distribution

of K_t by μ_t and the average capital by $S_t = \int k \mu_t(dk)$. In this setting, the interest rate is given by $r_t = C S_t$. Given an initial capital distribution μ_0 , the mean-field game is the solution to the MV-FBSDE system:

$$\begin{cases} dK_t = \left((r_t - \delta) K_t - \frac{1}{Y_t} \right) dt + \sigma (\rho dW_t^0 + \sqrt{1 - \rho^2} dW_t), & K_0 \sim \mu_0, \\ dY_t = -((r_t - \delta) Y_t) dt + Z_t dW_t + Z_t^0 dW_t^0, & Y_T = -K_T. \end{cases} \quad (31)$$

The system implicitly describes the probability measure flow $\mu_t = \mathcal{L}(K_t | \mathcal{F}_t^0)$, and the dynamics of this forward-backward system depend on μ_t through $r_t = C S_t = C \mathbb{E}[K_t | \mathcal{F}_t^0]$. Note that the optimal consumption c_t^* can be written as a function of (t, K_t, r_t) . Moreover, from the optimal consumption we can derive the *marginal propensity to consume* (MPC), given by

$$\partial_K c_t^* = -\frac{1}{Y_t^2} \frac{Z_t}{\sigma}.$$

This function describes, as a function of time, wealth and interest rate, how a increase in wealth is allocated between savings and consumption.

3.3.2. Numerical simulation and parameters. The initial condition follows a normal distribution with mean 0.5 and standard deviation 0.5. The system parameters are $C = 1.5$, $\delta = 0.1$, and $\sigma = 0.1$. We plot solutions with and without common noise in Figures 4 and 5, respectively.

In Figures 6 and 7, we plot the marginal propensity to consume surface when subjected to common noise, as a function of the interest rate r_t and capital K_t , at time 0.5 and 0.9 respectively. Note that at time 0.5, MPC is increasing in K_t , but concave in r_t - the intuition being that higher interest rates increase the payoff of saving behavior. However, the effect of the interest rate is reduced as we approach the end of the time interval.

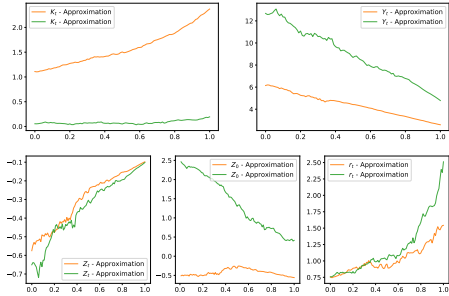


FIGURE 4. Numerical solution of economic growth model with common noise.

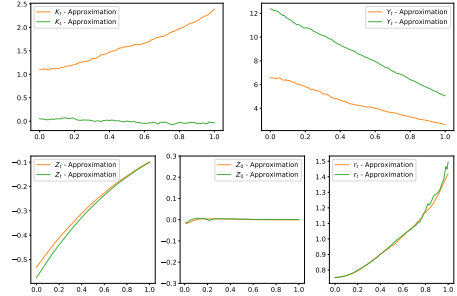


FIGURE 5. Numerical solution of economic growth model without common noise. Note that the model learns that Z_0 is irrelevant in this setting.

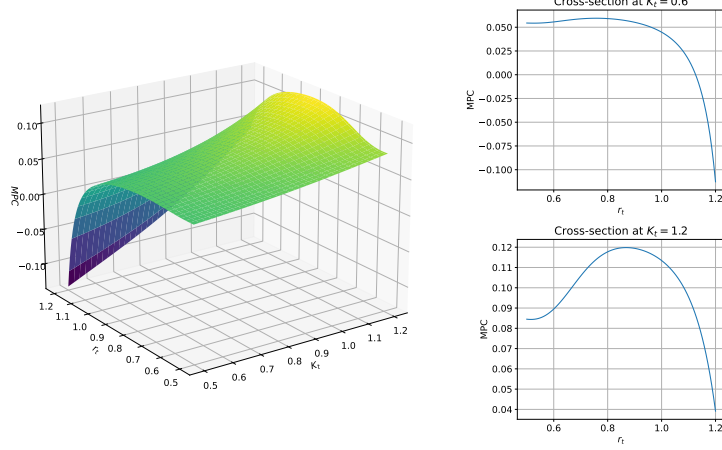


FIGURE 6. Marginal propensity to consume as a function of K_t and r_t , for time $t = 0.5$.

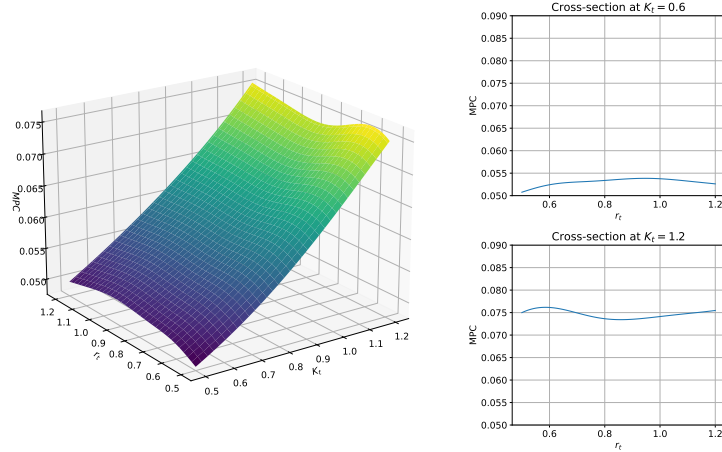


FIGURE 7. Marginal propensity to consume as a function of K_t and r_t , for time $t = 0.9$.

4. CONCLUSION

We have presented a novel numerical method for solving McKean-Vlasov forward-backward stochastic differential equations with common noise. Our approach combines Picard iterations with elicibility principles and deep learning to address the two fundamental challenges in these systems: the forward-backward coupling and the dependence on the conditional measure flow. The key innovation of our method lies in the use of elicibility to compute conditional expectations, which enables us to handle the common noise case without resorting to computationally expensive nested Monte Carlo simulations.

Our numerical experiments demonstrate the effectiveness of the proposed method across problems of varying complexity. The systemic risk banking model provides validation against known analytical solutions, confirming that our algorithm accurately recovers the true solution processes. The extension to quantile-mediated interactions showcases the flexibility of the elicibility framework in handling statistics beyond conditional means. Finally, the economic growth model illustrates the method's applicability to more complex, economically meaningful problems where analytical solutions are unavailable.

ACKNOWLEDGMENTS

SJ would like to acknowledge support from the Natural Sciences and Engineering Research Council of Canada through grant RGPIN-2024-04317. YS was supported by FAPERJ (Brasil) through the Jovem Cientista do Nossa Estado Program (E-26/201.375/2022 (272760)) and by CNPq (Brasil) through the Productivity in Research Scholarship (306695/2021-9). FA was supported by CAPES (Brazil) through Programa Institucional de Internacionalização (88887.939145/2024-00) and Programa Suporte à Pós-Graduação (88887.705168/2022-00), by FGV's School of Applied Mathematics and by UoT through a Research Assistant Award.

REFERENCES

- [CFS15] Rene A Carmona, Jean Pierre Fouque, and Li Hsien Sun. “Mean field games and systemic risk”. In: *Communications in Mathematical Sciences* 13.4 (2015), pp. 911–933.
- [FZ16] Tobias Fissler and Johanna F Ziegel. “Higher order elicibility and Osband’s principle”. In: (2016).
- [CD+18] René Carmona, François Delarue, et al. *Probabilistic theory of mean field games with applications I-II*. Springer, 2018.
- [CCD19] Jean-François Chassagneux, Dan Crisan, and François Delarue. “Numerical method for FBSDEs of McKean–Vlasov type”. In: *The Annals of Applied Probability* 29.3 (2019), pp. 1640–1684.
- [Lau21] Mathieu Lauriere. “Numerical methods for mean field games and mean field type control”. In: *Mean field games* 78.221-282 (2021).
- [Ach+22] Yves Achdou, Jiequn Han, Jean-Michel Lasry, Pierre-Louis Lions, and Benjamin Moll. “Income and wealth distribution in macroeconomics: A continuous-time approach”. In: *The Review of Economic Studies* 89.1 (2022), pp. 45–86.
- [GMW22] Maximilien Germain, Joseph Mikael, and Xavier Warin. “Numerical resolution of McKean–Vlasov FBSDEs using neural networks”. In: *Methodology and Computing in Applied Probability* 24.4 (2022), pp. 2557–2586.
- [Che+23] Jared Chessari, Reiichiro Kawai, Yuji Shinozaki, and Toshihiro Yamada. “Numerical methods for backward stochastic differential equations: A survey”. In: *Probability Surveys* 20 (2023), pp. 486–567.
- [CJC23] Anthony Coache, Sebastian Jaimungal, and Álvaro Cartea. “Conditionally elicitable dynamic risk measures for deep reinforcement learning”. In: *SIAM Journal on Financial Mathematics* 14.4 (2023), pp. 1249–1289.
- [HHL24] Jiequn Han, Ruimeng Hu, and Jihao Long. “Learning high-dimensional McKean–Vlasov forward-backward stochastic differential equations with general distribution dependence”. In: *SIAM Journal on Numerical Analysis* 62.1 (2024), pp. 1–24.

- [Pes+24] Silvana M Pesenti, Sebastian Jaimungal, Yuri F Saporito, and Rodrigo S Targino. “Risk budgeting allocation for dynamic risk measures”. In: *Operations Research* (2024).
- [ZOL24] Mo Zhou, Stanley Osher, and Wuchen Li. “A deep learning algorithm for computing mean field control problems via forward-backward score dynamics”. In: *arXiv preprint arXiv:2401.09547* (2024).